Materials Science & Engineering A 620 (2015) 445–453

Contents lists available at ScienceDirect

Materials Science & Engineering A

journal homepage: www.elsevier.com/locate/msea

Effect of interfacial reaction on age-hardening ability of B_4C/6061Al composites

Y.Z. Li [a], Q.Z. Wang [b,*], W.G. Wang [a], B.L. Xiao [a], Z.Y. Ma [a,**]

[a] Shenyang National Laboratory for Materials Science, Institute of Metal Research, Chinese Academy of Sciences, 72 Wenhua Road, Shenyang 110016, China
[b] Key Laboratory of Nuclear Materials and Safety Assessment, Institute of Metal Research, Chinese Academy of Sciences, 72 Wenhua Road, Shenyang 110016, China

ARTICLE INFO

Article history:
Received 3 July 2014
Received in revised form
4 October 2014
Accepted 12 October 2014
Available online 18 October 2014

Keywords:
Composites
Aluminum alloys
Age hardening
Hardness
Interfaces
Mechanical properties

ABSTRACT

The age-hardening ability of B_4C/6061Al composites, fabricated by powder metallurgy technique, were systematically investigated through varying B_4C contents (0–30 wt%), hot-pressing temperatures (560–620 °C) and holding times (30–120 min). The results showed that the quantity of Mg_2Si precipitates formed in the composites after T6-treatment decreased with increasing B_4C content and hot-pressing temperature, attributable to the consumption of Mg resulting from interfacial reactions. The main interfacial reaction products were $MgAl_2O_4$ and Al_3BC. The formation of $MgAl_2O_4$ was determined to be the primary factor degrading the age-hardening ability of the composites. Reducing the hot-pressing temperature and holding time and increasing the Mg content were beneficial to improving the age-hardening ability of the composites. It was experimentally verified that 580 °C and 30 min were the optimal hot-pressing temperature and holding time, and the amount of additional Mg should be less than 1.5 wt%, when considering both the age-hardening ability and comprehensive properties of the composites.

1. Introduction

Aluminum matrix composites (AMCs) have received significant attention as candidate materials for aerospace and automotive applications in recent years. Generally, AMCs have higher specific modulus, strength, wear resistance and elevated-temperature resistance than unreinforced alloys [1,2]. As a kind of new reinforcement, B_4C has the lowest density (about 2.52 g/cm^3) among ultrahard materials, and its hardness (9.5+ in Mohs' scale) is just below that of the diamond and c-BN. Also, B_4C exhibits similar thermal expansion coefficient, thermal stability and chemical inertness to SiC. Thus, B_4C becomes an alternative to SiC and Al_2O_3 for fabricating advanced AMCs with high stiffness, good wear resistance and impact resistance [3,4]. In addition, the specific ability of the B-10 isotope to capture neutrons makes the B_4C/Al composite an ideal neutron absorbing material in nuclear industries [5,6].

Commercial Al alloys are usually used as the matrices of AMCs because of their low cost and availability. For the AMCs with heat treatable Al alloys as the matrices, the mechanical properties could be significantly modified through heat treatment [7,8]. Aging is a common heat treatment method to improve the mechanical properties of AMCs. The age-hardening behavior of AMCs has been the subject of a number of investigations.

Appendino et al. [9] compared the aging behavior of 6061Al and 14 vol%SiC/6061Al composite. It was reported that the aging behavior of the composite was similar to that of the matrix, although accelerated aging kinetics was observed for the composite. The similarity of the aging behavior between the composites and the matrix alloys was also observed by Chu [10] and Dutta et al. [11]. A theoretical model was developed by Dutta et al. to predict the rate of precipitation. In summary, the age-hardening behavior of AMCs is mainly controlled by the characteristics of the matrix alloys and the optimum aging parameters have already been obtained for some common AMCs in previous studies [9–13].

In addition to the characteristics of the matrixes, the interface reactions would also affect the aging behavior of the composites. Especially, those reactions involving the alloy elements would change the composition of the matrixes and consequently change the age-hardenability of the composites [14–18]. For some composite systems, these reactions could enhance the age-hardening ability of the composites. For example, in an Al–Mg–SiC system, the reactions between Al and SiC increased the Si content in the matrix alloy, leading to a modified age-hardening ability of the composite, though the increment was not significant [14]. For some other composite systems, these reactions would deteriorate the age-hardening ability of the composites. For example, in an

* Corresponding author. Tel./fax: +86 24 23971749.
** Corresponding author. Tel./fax: +86 24 83978908.
E-mail addresses: qzwang@imr.ac.cn (Q.Z. Wang), zyma@imr.ac.cn (Z.Y. Ma).

http://dx.doi.org/10.1016/j.msea.2014.10.025
0921-5093/

Al–Mg–Si–Al_2O_3 system, the reaction between Mg and Al_2O_3 resulted in the consumption of Mg, degrading the age-hardening ability of the composite [15].

As for the Al–B_4C system, very few studies reported on the interfacial reactions involving alloy elements and their effects on the aging behavior of the composites. Some investigations mentioned that Mg involved reactions possibly produced negative impact on the age-hardening ability of B_4C/Al composites, but did not provide experimental evidences and detailed analyses [18].

For 6061Al-based composites, the age-hardening ability may be easily affected by the addition of reinforcements because of low content of the alloy elements Mg and Si. Although the aging behavior of 6061Al-based composites was reported in some studies [19,20], most of these studies focused on the aging kinetics and did not account for the effects of the reinforcement on the age-hardening ability of these composites. To the best of our knowledge, investigation of aging behavior of B_4C/6061Al composites is lacking up to this point.

In the present study, B_4C/6061Al composites were fabricated by powder metallurgy (PM) technique. The effect of B_4C on the age-hardening ability of B_4C/6061Al composites was systematically investigated through varying the B_4C contents (0–30 wt%), hot-pressing temperatures (560–620 °C) and holding times (30–120 min). The aim is to elucidate the effect of interfacial reaction on the age-hardening ability of B_4C/6061Al composites.

2. Experimental

B_4C/6061Al composites were fabricated by PM technique using 6061Al alloy with a nominal composition of Al–1.0 Mg–0.65Si–0.25Cu (wt%) as the matrix and B_4C as the reinforcement. The mean sizes of aluminum powders and B_4C particles were 13 and 7 μm, respectively. The as-received B_4C particles were dried at 150 °C for 8 h, and then mechanically mixed with the Al powders for 8 h in a bi-axis rotary mixer with a rotation speed of 50 rpm and a ball to powder ratio of 2:1. The as-mixed powders were cold pressed in a cylindrical die under a pressure of 50 MPa and then hot pressed under a pressure of 30 MPa, producing the composite billets 55 mm in diameter and 60 mm in height. For comparison, unreinforced 6061Al alloy was also fabricated under the same fabrication conditions.

In order to clarify the key factors influencing the interfacial reactions and age-hardening ability separately, three series experiments were designed in the present study, as following:

(I) B_4C/6061Al composites reinforced with 0, 15, 20, 25 and 30 wt% B_4C particles were hot pressed at 620 °C with a holding time of 120 min to investigate the effect of B_4C content on the age-hardening ability (Section 3.2). 620 °C is between the solidus and liquidus of the matrix alloy and can ensure the occurrence of partial liquid phase during the fabrication of the composites.

(II) 20 wt%B_4C/6061Al composites were fabricated at 560, 580, 600 and 620 °C to investigate the effect of the hot-pressing temperature on the age-hardening behavior. Furthermore, 20 wt%B_4C/6061Al composites hot-pressed at 620 °C with different holding times of 30, 60, 120 min were also fabricated to investigate the effect of holding time on the age-hardening behavior (Section 3.3).

(III) 20 wt%B_4C/6061Al composites with different extra Mg additions (0, 0.5, 1, 1.5 wt%) were fabricated at a hot pressing temperature of 620 °C and a holding time of 120 min to investigate the influence of Mg content on the age-hardening ability (Section 3.4).

To reduce the defects and enhance the mechanical properties, all the hot-pressed billets were hot forged at 480 °C into disc plates 12 mm in thickness and then subjected to the microstructural examinations and property tests. The densities of the composites were measured using the Archimedes principle. The microstructures and phase compositions were examined and analyzed by scanning electron microscopy (SEM, quanta 600) and X-ray diffraction analyzer (D/max 2400). Semi-quantitative analysis was also performed to evaluate the variation of the relative abundances of the phases. For each characterized phase, the evaluation was realized by measuring the intensities of three characteristic diffraction lines free of overlap and by comparing the obtained values from one sample to another. Differential scanning calorimetry (DSC TA-Q1000) was conducted in the flowing argon atmosphere with a heating rate of 10 °C/min. Small pieces of specimens (50 mg) were cut from the powder compacts which were hot pressed at a lower temperature of 400 °C to ensure enough densification and restrain interfacial reactions and element diffusion.

Age hardening behavior of the composites and matrix alloy were characterized using the Brinell hardness measurement under both as-solutionized (solution treated at 530 °C for 2.5 h, water quenched) and peak-aged (T6, solution treated at 530 °C for 2.5 h, water quenched, and then aged at 175 °C for 6 h) conditions. Six specimens per condition were measured to ensure the accuracy of results. Dogbone-shaped tensile specimens (25 mm gage length, 4 mm gage width and 2 mm gage thickness) were electrical discharge machined from the forged disc plate. Tensile tests were conducted under T6 condition using an INSTRON 5582 tester at a strain rate of 10^{-3} s^{-1}. The property values for each condition were calculated by averaging three test results.

3. Results

3.1. B_4C particles

Fig. 1 shows the SEM micrograph and the XRD pattern of the B_4C particles. It is noted that the B_4C particles exhibited a polygonal morphology with blunt edges and small aspect ratios

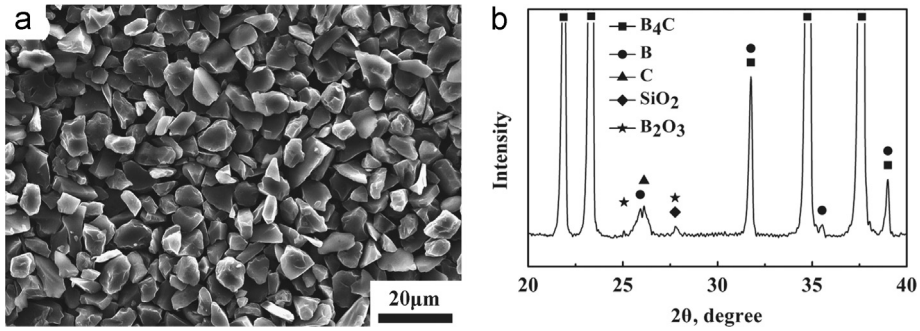

Fig. 1. (a) SEM micrograph and (b) XRD pattern of as-received B_4C particles.

(Fig. 1(a)). It seems that the surfaces of the particles were very clean without obvious impurities. However, the XRD pattern indicated the existence of a few impurities, such as free B and C, SiO_2 and B_2O_3 in the B_4C particles (Fig. 1(b)).

3.2. B_4C/6061Al composites with various B_4C contents hot pressed at 620 °C for 120 min

Table 1 shows the densities of the forged B_4C/6061Al composites and 6061Al alloy. The results indicated that all the composites with various B_4C contents and the 6061 alloy were almost completely densified. As shown in Fig. 2, for all the composite samples, the B_4C particles exhibited uniform distribution in the matrix, especially in the composites with the B_4C contents of 15 and 20 wt% (Fig. 2(a) and (b)). Even for the composites with higher B_4C contents (25 and 30 wt%) the distribution of the particle was still uniform, although inconspicuous clusters less than 30 μm began to appear (Fig. 2(c) and (d)). Furthermore, no macro-pores were observed in all the composites.

Fig. 3 shows the SEM micrographs of the forged B_4C/6061Al composites with various B_4C contents. It can be clearly seen that the morphology of B_4C particles in the composites was different from that of the as-received B_4C. The cusps of the particles were obviously blunted and the even and sharp edges of the particles were serrated in all the composites. This indicates that interfacial reaction occurred between B_4C and the matrix. However, no reaction product could be identified under SEM. The white particles pointed out by white arrows were identified to be B_4C by energy dispersive spectrometer (EDS) analysis, too. It is important to note from Fig. 3 that the degree of B_4C being attacked decreased with the increase of the B_4C contents from 20 to 30 wt%.

Table 1
The densities of forged B_4C/6061Al composites with various B_4C contents hot pressed at 620 °C and forged 20%B_4C/6061Al composites hot pressed at various temperatures with a holding time of 120 min.

Samples	Measured density, g/cm^3	Theoretical density, g/cm^3	Relative density, %
Content of B_4C, wt%			
0	2.706	2.70	100.22
15	2.676	2.67	100.20
20	2.667	2.66	100.23
25	2.646	2.65	99.80
30	2.637	2.64	99.89
Hot-pressing temperature, °C			
560	2.642	2.66	99.32
580	2.643	2.66	99.36
600	2.657	2.66	99.89
620	2.665	2.66	100.19

Fig. 4 shows the XRD patterns of the forged B_4C/6061Al composites with B_4C contents of 0, 15 and 20 wt%. It can be seen that the predominant phases were Al or/and B_4C, with much higher intensities in all the XRD patterns. Apart from Al, only Mg_2Si peaks occurring in (111) and (220) planes could be observed in the 6061Al alloy, which was the primary strengthening phase in the 6061Al alloy. However, the intensities of the Mg_2Si peaks were too weak to be detected in the composites compared with the 6061Al alloy, especially when the content of B_4C was up to 20 wt%. Instead of Mg_2Si, an Mg containing phase, $MgAl_2O_4$, which was overlapped with the Al_3BC or C peaks, was detected in the composites. Furthermore, Al_3BC, a possible interfacial reaction product between Al and B_4C, was also detected in the composites. It is noted from Fig. 4 that some peaks with very low intensities could not be affirmed only by XRD patterns because of the interference and overlap with other peaks.

To evaluate the changing tendency of Al_3BC and Mg_2Si with the B_4C content in the composites, based on the relative intensity of Al (111), Al_3BC (101), Mg_2Si (220) and B_4C (104) planes, the relative intensity fractions of the Al_3BC and Mg_2Si in the forged B_4C/6061Al composites reinforced with 0, 15 and 20 wt% B_4C particles were calculated by following equation, according to Ref. [21].

$$D_X(\%) = \frac{I_X}{I_{Al} + I_X + I_{B_4C}}(\%) \quad (1)$$

where D_x is the relative intensity fraction of compound x (Al_3BC or Mg_2Si), I_{Al} and I_{B4C} are the intensities of Al and B_4C, respectively, and I_x are the intensity of compound x. The calculated results are

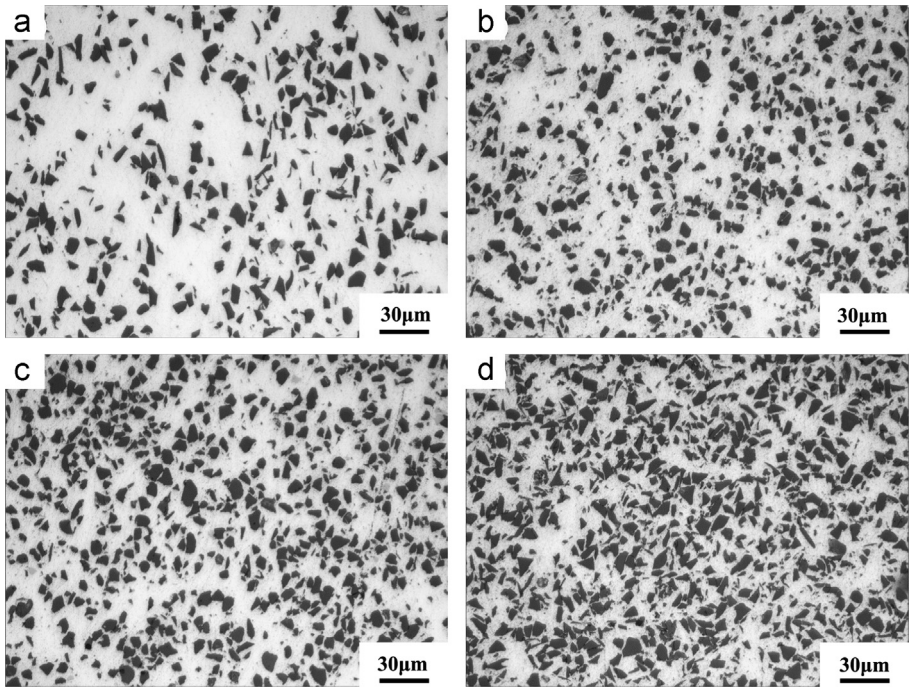

Fig. 2. Optical micrographs of forged B_4C/6061Al composites with various B_4C contents hot pressed at 620 °C with a holding time of 120 min: (a) 15 wt%, (b) 20 wt%, (c) 25 wt%, and (d) 30 wt%.

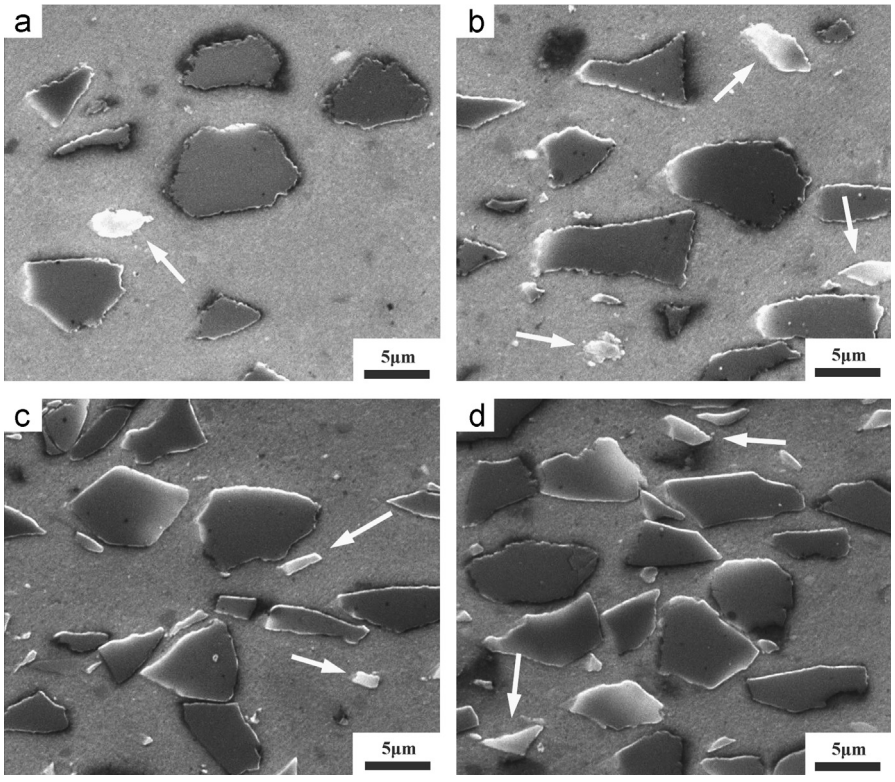

Fig. 3. SEM micrographs of forged B_4C/6061Al composites with various B_4C contents hot pressed at 620 °C with a holding time of 120 min: (a) 15 wt%, (b) 20 wt%, (c) 25 wt%, and (d) 30 wt%.

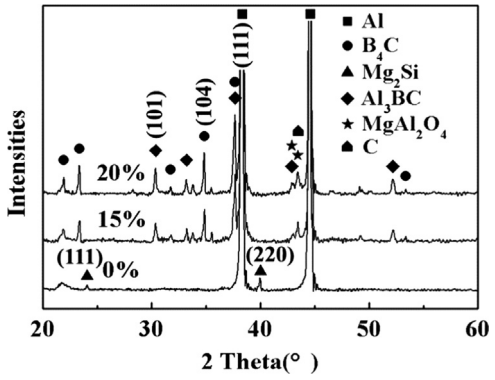

Fig. 4. XRD patterns of forged B_4C/6061Al composites with various B_4C contents hot pressed at 620 °C with a holding time of 120 min.

listed in Table 2. It can be seen that the amount of Al_3BC increased with the increase of B_4C content in the composites, while the amount of Mg_2Si decreased. Because the peaks of $MgAl_2O_4$ were overlapped with the Al_3BC or C peaks, it was hard to calculate the relative intensity fractions by means of Eq. (1). However, it can be seen from the XRD patterns (Fig. 4) that the intensities of $MgAl_2O_4$ peaks increased slightly in the composites when the content of B_4C increased from 15 to 20 wt%.

Fig. 5 shows the variation of hardness of the B_4C/6061Al composites with the B_4C content under both peak-aged and as-solutionized conditions. Inspection of Fig. 5 leads to four significant findings. First, the presence of the B_4C particles produced a marked hardening of the composites in the as-solutionized condition. The monolithic alloy exhibited a hardness of 43 HBS, whereas the composites showed the hardness values from 70 to 100 HBS, and the hardness of the composites increased near-linearly with the contents of B_4C. Second, both the composites

Table 2
The relative intensity fractions of primary phases calculated based on Al (111), Al_3BC (101), Mg_2Si (220) and B_4C (104) in the forged 0, 15 and 20 wt%B_4C/6061Al composites hot pressed at 620 °C with a holding time of 120 min.

Content of B_4C, wt%	Relative fraction (%)	
	Al_3BC	Mg_2Si
0	0	0.71
15	1.16	0.24
20	1.54	0.08

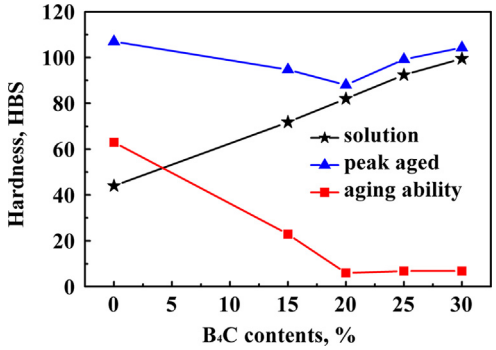

Fig. 5. Age-hardening ability of forged B_4C/6061Al composites with various B_4C contents hot pressed at 620 °C with a holding time of 120 min.

and the monolithic alloy exhibited an age-hardening behavior. The hardness of all the materials increased after the artificial aging, but in different degrees. Third, the age-hardening ability of the composites, which was defined as a difference between peak-aging hardness and solution hardness as shown in Fig. 5, was severely decreased in comparison with the monolithic alloy.

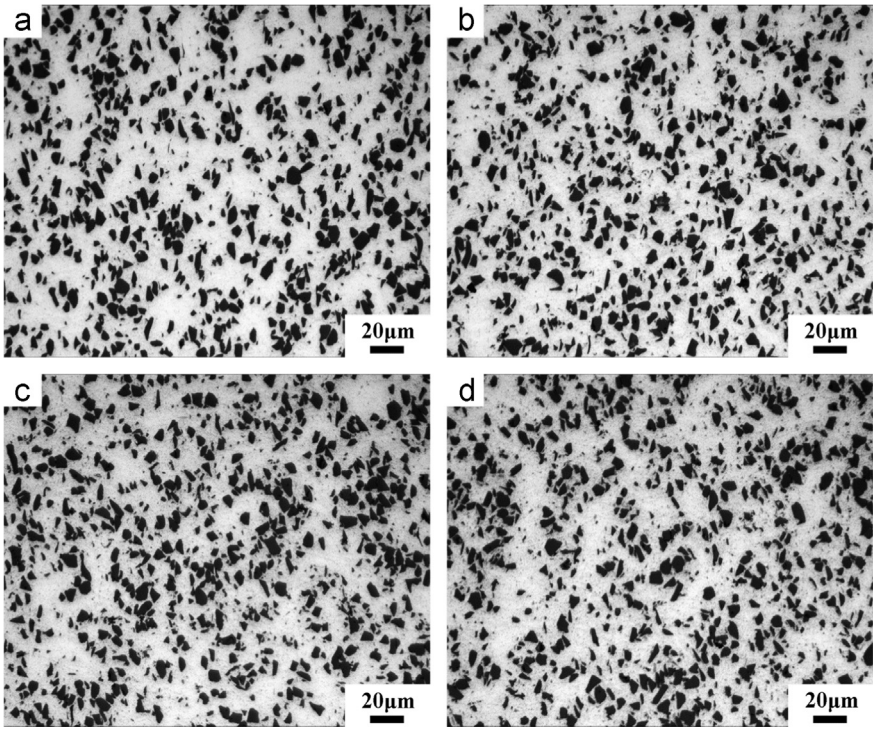

Fig. 6. Optical micrographs of forged 20 wt%B_4C/6061Al composites with various hot-pressing temperatures: (a) 560 °C, (b) 580 °C, (c) 600 °C, and (d) 620 °C.

Especially when the contents of B_4C were up to 20 wt%, the age-hardening ability of the composites was almost negligible, only about 5 HBS in hardness increase. By comparison, the age-hardening ability of the monolithic alloy was more than 60 HBS. Fourth, in the peak-aged condition, the hardness of the composites decreased with increasing B_4C contents before reaching the minimum at 20 wt% and then increased. The hardness and the age-hardening ability of all the composites were inferior to those of the monolithic alloy in the peak-aged condition.

3.3. *B_4C/6061Al composites with various hot-pressing temperatures*

As shown in Table 1, the densities of the forged 20 wt%B_4C/6061Al composites slightly increased with increasing hot-pressing temperature. It can be seen that it was easy to achieve complete densification when the hot-pressing temperature was above 600 °C.

Fig. 6 shows the optical micrographs of the forged 20 wt%B_4C/6061Al composite with various hot-pressing temperatures. For all the composites, the B_4C particles exhibited uniform distribution in the matrix. Furthermore, no macro-pores were observed in all the composites.

Fig. 7 shows the SEM micrographs of the forged 20 wt%B_4C/6061Al composites with various hot-pressing temperatures. It can be clearly seen that the morphology of B_4C particles and the microstructure of the matrix were different for different hot-pressing temperatures. When the temperatures were lower than 600 °C, the morphology of B_4C particles was similar to that of the as-received ones, and the matrix was clean (Fig. 7(a–d)). However, when the temperature increased to 600 °C, the morphology of B_4C particles started to change and some gray phases appeared in the matrix, as indicated by the white arrows in Fig. 7(f) and (h). These gray phases were identified to be rich in Mg by EDS. It is noted that the degree of B_4C being attacked and the amount of the Mg rich phases significantly increased with the increase of the hot-pressing temperature from 600 to 620 °C (Fig. 7(e–h)).

Fig. 8 shows the XRD patterns of the forged 20 wt%B_4C/6061Al composites with various hot-pressing temperatures. The Mg_2Si peaks occurring in (111) and (220) planes could be observed clearly in the composites hot pressed at 560, 580 and 600 °C. However, the intensities of the Mg_2Si peaks were too weak to be detected in the composite hot pressed at 620 °C. Except Mg_2Si, Al_3BC and $MgAl_2O_4$ were detected in all the composites. Meanwhile, some tiny peaks were also detected but could not be affirmed only by XRD patterns. The relative intensity fractions of the Al_3BC and Mg_2Si in the composites with different hot-pressing temperatures were calculated by Eq. (1), and are listed in Table 3.

It can be seen that the amount of Al_3BC was negligible at the hot-pressing temperature of 560 °C and increased with the hot-pressing temperature, while the amount of Mg_2Si decreased continuously. The increase of Al_3BC and the decrease of Mg_2Si were slight when the temperature increased from 560 to 580 °C. However when the temperature raised to 600 °C or higher, the increase of Al_3BC and decrease of Mg_2Si were significant, especially when the temperature increased from 600 to 620 °C. Because the peaks of $MgAl_2O_4$ were overlapped with other phases, the relative intensity fractions could not be calculated by Eq. (1). However, it can be seen from Fig. 8 that the intensities of $MgAl_2O_4$ peaks were tiny and almost the same at the hot-pressing temperatures of 560 and 580 °C, while they increased obviously when temperature continued to increase.

According to the XRD results above, two different temperature ranges could be distinguished concerning the interface reactions of the B_4C/6061Al composites. First, at hot-pressing temperatures lower than 600 °C, all the reactions were slight and the amount of the reaction products showed a very slight increase with the temperature in this range. Second, at hot-pressing temperatures higher than 600 °C, the interfacial reactions were severe and the amount of the reaction products showed an obvious increase with the temperature.

Fig. 9(a) shows the age-hardening ability of the forged 20 wt% B_4C/6061Al composites with various hot-pressing temperatures. It can be seen that with the rise of the hot-pressing temperature, two significant changes could be observed for the composites. First, the hardness of the composites at the as-solutionized

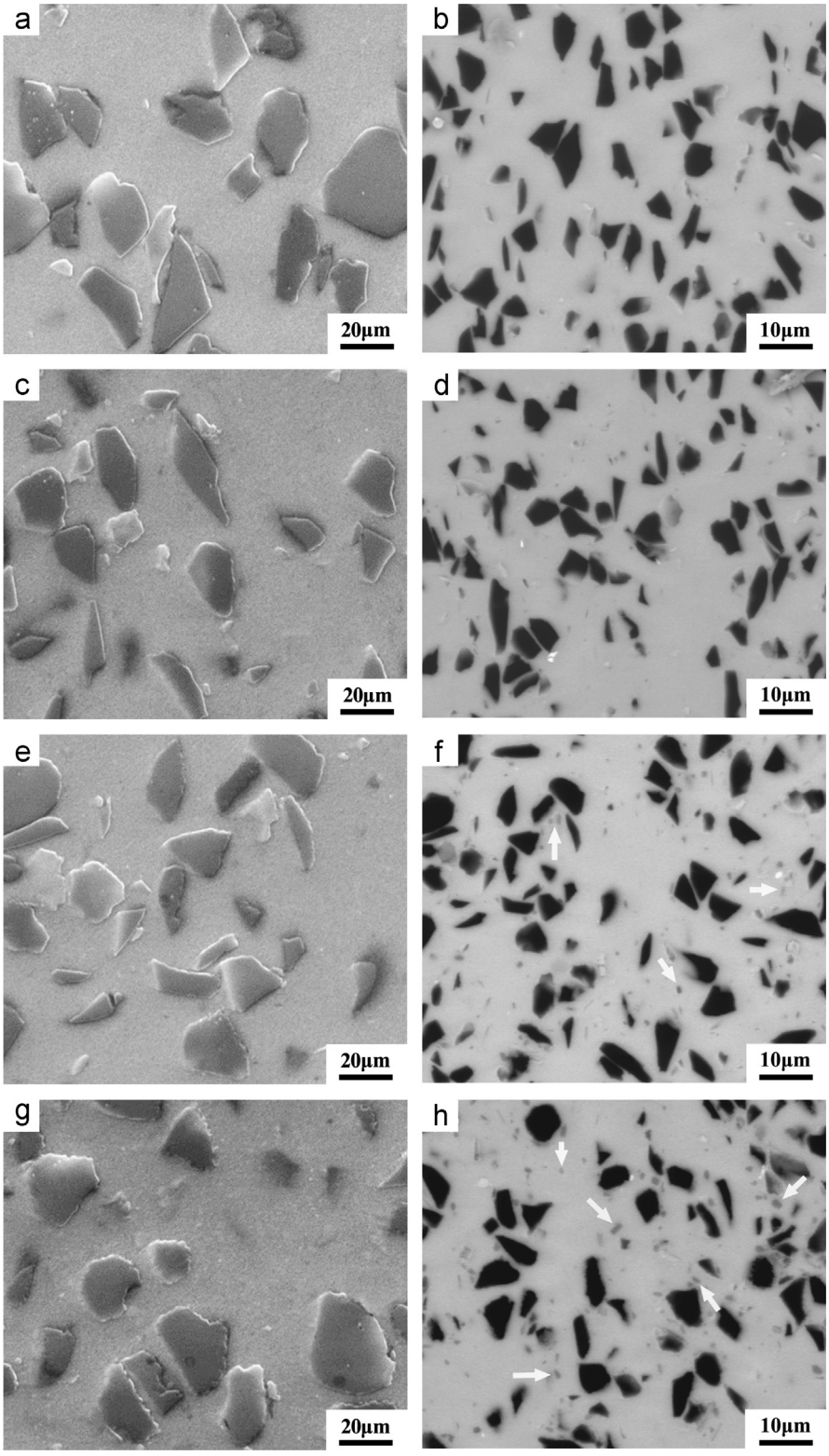

Fig. 7. SEM micrographs of forged 20 wt%B_4C/6061Al composites with various hot-pressing temperatures: (a, b) 560 °C, (c, d) 580 °C, (e, f) 600 °C, and (g, h) 620 °C.

condition exhibited very slight decrease as the hot-pressing temperature increased from 560 to 620 °C. Second, the age-hardening abilities of the composites were at the same level when the hot-pressing temperatures were 560 and 580 °C. However, the age-hardening ability showed a continuous decrease with the hot-pressing temperature rising from 580 to 620 °C.

Fig. 9(b) shows the tensile properties of the forged 20 wt%B_4C/6061Al composites under T6 condition with various hot-pressing temperatures. It can be seen that the variation tendency of the strength was basically consistent with that of the hardness. However, unlike the hardness, the strength of the 20 wt%B_4C/6061Al composites slightly increased when the hot-pressing temperature increased from 560 to 580 °C. It may be ascribed to more sufficient element diffusion at 580 °C, leading to a stronger interface bonding of B_4C/Al and Al/Al particles. Therefore, 580 °C was selected as the optimized hot-pressing temperature for the

B_4C/6061Al composites considering both the interface bonding and the interface reactions.

3.4. B_4C/6061Al composites with various hot-pressing holding times

The interfacial reaction of the 20 wt%B_4C/6061Al composites at the hot-pressing temperature of 620 °C were proven to be severer than that at lower temperatures and the age-hardening ability of the composite hot pressed at 620 °C with a holding time of 120 min almost disappeared. However, 620 °C was a proper hot-pressing temperature for the densification of the composites due to the presence of partial liquid. In order to reduce the interfacial reaction, it is necessary to study the influence of the holing time at 620 °C on the age-hardening ability of the 20 wt%B_4C/6061Al composites.

Fig. 10 shows the age-hardening ability of the forged 20 wt% B_4C/6061Al composites with various holing times at 620 °C. It can be seen that with the prolongation of the holding time, two significant changes were observed. First, the hardness of the as-solutionized composite decreased slightly with the prolongation of the holding time, while the peak-aging hardness decreased significantly, resulting in markedly decreased age-hardening ability. This is attributed to increased depletion of Mg with increasing interfacial reaction time. Second, the decrease rate of the age-hardening ability was very high when the holding time was prolonged from 30 to 60 min and then became slow with further increasing the holding time to 120 min.

3.5. B_4C/6061Al composites with various contents of additional Mg

Fig. 11 shows the age-hardening ability of the forged 20 wt% B_4C/6061Al composites with various amounts of additional Mg. With the addition of the additional Mg, three significant changes can be observed. First, the hardness of the as-solutionized composites increased slightly and near-linearly with the additional Mg contents. Second, the additional Mg definitely recovered the age-hardening ability of the B_4C/6061Al composites. The age-hardening ability of the composite with 1.5 wt% additional Mg hot-pressed at 620 °C (45 HBS) basically matched that of the 20 wt% B_4C/6061Al composites hot-pressed at 580 °C (44 HBS). Third, the age-hardening ability of the composites increased with the

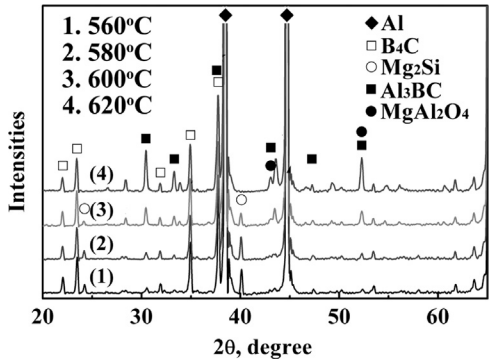

Fig. 8. XRD patterns of forged 20 wt%B_4C/6061Al composites with various hot-pressing temperatures.

Table 3
The relative intensity fractions (%) of primary phases calculated based on Al (111), Al_3BC (101), Mg_2Si (220) and B_4C (104) in forged 20 wt%B_4C/6061Al composites hot pressed at various temperatures with a holding time of 120 min.

Hot-pressing temperature, °C	560	580	600	620
Al_3BC	0.27	0.31	0.75	1.54
Mg_2Si	0.98	0.93	0.52	0.08

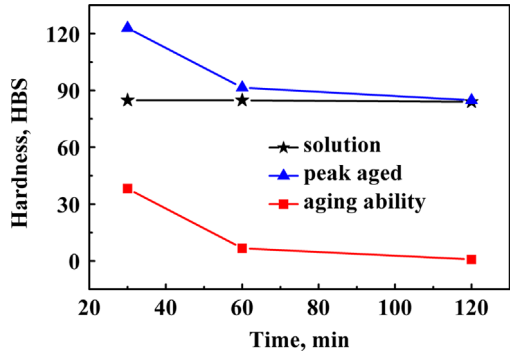

Fig. 10. Age-hardening ability of forged 20 wt%B_4C/6061Al composites with various holding times at 620 °C.

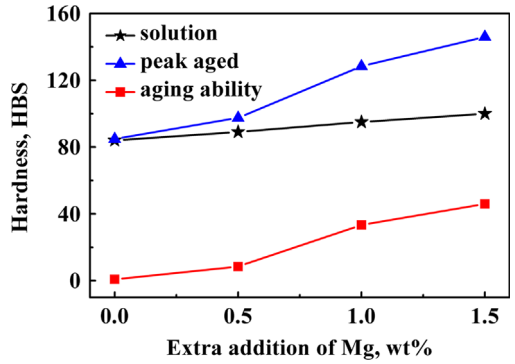

Fig. 11. Age-hardening ability of forged 20 wt%B_4C/6061Al composites with various contents of additional Mg.

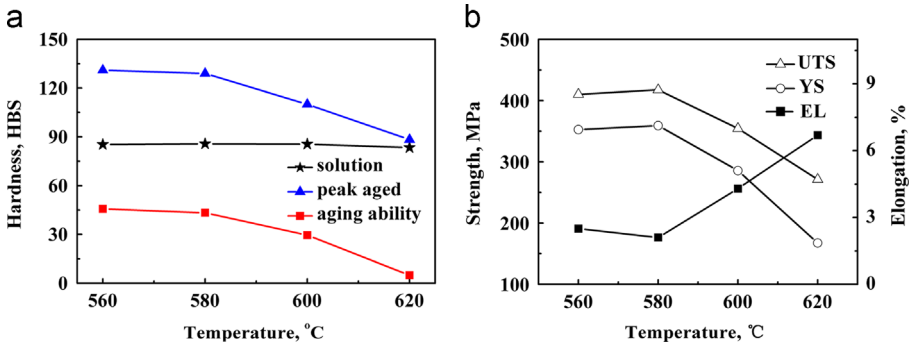

Fig. 9. (a) Age-hardening ability and (b) tensile properties (T6) of forged 20 wt%B_4C/6061Al composites with various hot-pressing temperatures.

additional Mg contents in a parabolic pattern, with the maximum increment at 1.0 wt% and the minimum at 0.5 wt%.

4. Discussion

4.1. Interface reactions

4.1.1. Reaction temperature range

It was well known that the existence of a liquid phase would definitely accelerate the rate of reactions occurring in material systems [22]. Fig. 12 shows the DSC curves of the 6061Al–B_4C and Al–B_4C powder mixtures after being hot pressed at 400 °C. The hot pressing of the powders at a lower temperature was used to ensure the close contact of the particles with each other to produce the sufficient element diffusion in the DSC test. This test was designed as a simulation of the phase changes with the temperature during the hot-pressing process. It can be seen from Fig. 12 that different from Al–B_4C, the melting commencement temperature of the 6061Al–B_4C powder mixtures was reduced to 600 °C.

In this study, two different temperature ranges with the boundary being 600 °C could be determined based on the interface reactions of the B_4C/6061Al composites. This boundary is closely related to the appearance of the liquid phase in the B_4C/6061Al composites according to the DSC result. With the rise of the hot-pressing temperature above 600 °C, the proportion of the liquid phase increased, causing a larger degree of element contact, which facilitated element diffusion and accelerated reaction rate in the composites. This would lead to the occurrences of severer interfacial reactions and the formation of larger amount of reactive products. Therefore, all the experiment phenomena in the present study were divided into two parts with 600 °C as the critical temperature.

4.1.2. Reaction between Al and B_4C

The reaction between Al and B_4C has already been proven by some researchers [3,4,23]. Although it is difficult to react with aluminum in solid state, B_4C has been proven to be unstable in melt aluminum. Al_3BC has also been confirmed as the main reaction product when the reaction temperature ranges from 627 to 800 °C. Though the fabrication temperature of the composites was lower than 627 °C in the present study, and much lower than the temperature for the complete melting of the matrix alloy, partial melting already occurred during the hot-pressing of the composites when the hot-pressing temperature rose to 600 °C as discussed in Section 4.1.1. As a result, interfacial reactions between Al and B_4C would occur at 600 °C or higher, leading to the generation of Al_3BC as shown in Fig. 8 and the change of the morphology of B_4C particles as shown in Fig. 7(e) and (g).

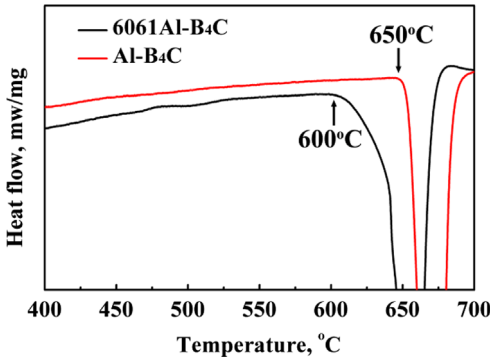

Fig. 12. The DSC curves of 6061Al–B_4C and Al–B_4C powder mixtures after cold pressing.

With the increase of temperature, the ratio of the liquid phase in the composites increased. This would facilitate the reactions between the reinforcement and the metal matrix due to the increase of opportunity for the reinforcement to contact with the alloy melt and the acceleration of the element diffusion. Consequently, the erosion degree of the B_4C particles aggravated and the amount of the Al_3BC in the composites increased.

With the increase of the reinforcement contents, the ratio of the metal matrix in the composite would decrease. Correspondingly, the ratio of the liquid phase in the composites would also decrease. The Al/B_4C reaction would generate B element into the liquid phase. Because of the very low solubility of B in the Al liquid, the Al/B_4C reaction would be suppressed. The less ratio of the liquid, the larger extent of the suppression would occur. This may be a reason that the degree of the B_4C being eroded by interface reactions decreased with the increase of the B_4C contents from 20 to 30 wt% as shown in Fig. 3 in the present study.

4.1.3. Reaction between Mg and the oxides

The formation of $MgAl_2O_4$ has been reported in the B_4C/Al composites with different matrix alloys as well as in SiC/Al and Al_2O_3/Al composite systems [2,22]. On the one hand, O element could be brought into the composites from many resources. XRD analysis revealed the presence of B_2O_3 in the as-received B_4C particles (Fig. 1(b)). Another possible source of O element in the composites could be the Al_2O_3 film on the Al particles and the moisture adsorbed onto the powders. On the other hand, Mg element was expected to segregate naturally to the interfaces because of strong surface activity and substantial stress field near the interfaces. At a high hot-pressing temperature of 620 °C in the present study, the following reactions could take place in the composites [21,22]:

$$3Mg + B_2O_3 = 3MgO + 2B \quad (2)$$

$$3Mg + Al_2O_3 = 3MgO + 2Al \quad (3)$$

$$3Mg + 4Al_2O_3 = 3MgAl_2O_4 + 2Al \quad (4)$$

Reactions (2–4) would cause definitely assumption of Mg element in the matrix alloy, thereby leading to two microstructure changes in the composites. First, the Mg element would segregate to produce the Mg rich phases shown in Fig. 7(f) and (h)) and could not be distributed uniformly in the matrix even after solution treatment. Second, the amount of the formed Mg_2Si would decrease as shown in Figs. 4 and 8.

4.2. Age-hardening ability

The interface reactions involving Mg would lead to the segregation of Mg in the matrix. As a result, the weakened solution strengthening effect was observed after quenching of the composites. This was supported by the result that the solution hardness of the composites decreased slightly with increasing the hot-pressing temperatures as shown in Fig. 9(a).

The variation tendency of the age-hardening ability of the B_4C/6061Al composites with the hot-pressing temperature was in accordance with the interfacial reaction results as shown above. It is well known that Mg_2Si is essential for the age-hardening of 6061Al alloy. As mentioned above, distinct interfacial reactions would occur in the B_4C/6061Al composites. Furthermore, some of the reactions might occur between Mg and the oxides in the raw powders, including B_2O_3 and SiO_2 in B_4C powders (Fig. 1(b)), Al_2O_3 film on the surface of the Al powders and the moisture adsorbed onto the powder particles. This would transform Mg to $MgAl_2O_4$ and result in severe consumption of Mg in the matrix alloy. The consumption of Mg would decrease the amount of Mg_2Si

precipitates during the aging treatment of the composites, thereby deteriorating the age-hardening ability (Fig. 5).

The amount of Mg element in the 6061Al alloy is only 1 wt%. And the amount of the oxides in the raw B_4C and Al powders are also limited. Thus, the consumption of Mg element and the deterioration of the age-hardening ability would be related to the hot-pressing parameters and the B_4C or Mg contents in the composites. When the hot-pressing parameters were 620 °C and 120 min, the age-hardening ability of 15 wt%B_4C/6061Al composite was relatively higher compared with other composites. This may be attributed to the fact that not all the Mg element was consumed in the interfacial reactions between Mg and the oxides due to relatively low B_4C content, and a small amount of remaining Mg element could precipitate as Mg_2Si during the aging treatment to strengthen the composite, though the strengthening was much lower than that in the 6061Al alloy. When the content of B_4C was 20 wt% or more, the hardness increment after the aging treatment was negligible. The intensities of Mg_2Si peaks could also be neglected in the XRD patterns (Fig. 4). Therefore, it should be concluded that Mg element was completely consumed and the age-hardening ability disappeared in the 20 wt%B_4C/6061Al composites hot-pressed at 620 °C with a holding time of 120 min. This may be the opportune hot-pressing parameters and composition that cause the complete consumption of Mg and the disappearance of the age-hardening ability of the composites.

From Fig. 10, it can be concluded that the consumption amount of Mg was closely related with the holding time of the solution treatment. When the holding time was prolonged from 30 to 60 min at the hot-pressing temperature of 620 °C, most of Mg was consumed by the interfacial reactions, resulting in a rapid decrease in the hardness. With further prolonging the holding time to 120 min, only a small amount of remnant Mg was consumed. In this case, the deterioration rate in the age-hardening ability became slow with the holding time.

Based on above analyses, both the decrease of the B_4C contents, the hot-pressing temperature and the holding time, and the increase of the Mg contents should be beneficial to improving the age-hardening ability of the B_4C/6061Al composites. This is attributed to the suppression of Mg consumption resulting from interfacial reactions.

For PM fabrication, proper temperature and holding time are needed to ensure the sufficient sintering of the powders during the hot-pressing process. Usually, the holding time longer than 30 min should be utilized. Based on Figs. 9 and 10, 580 °C and 30 min are determined to be the optimal hot-pressing temperature and holding time for fabricating the B_4C/6061Al composites, when comprehensively considering the composite sintering and the interface reactions. The addition of more Mg would deteriorate the other properties of the composites such as workability. Therefore, additional Mg should not be more than 1.5 wt%, considering the negative impact and the remedy of the age-hardening ability.

In summary, the effect of the B_4C contents, the hot-pressing temperature and the holding time as well as the addition of additional Mg on the age-hardening ability have been clearly elucidated. However, some tiny peaks in the XRD patterns have not been affirmed and the interfacial reaction mechanism involving the formation of two types of different compounds Al_3BC and $MgAl_2O_4$ is still unclear. The research on these issues is under progress, and will be discussed in a subsequent publication.

5. Conclusions

1. In the B_4C/6061Al composites prepared by the PM method, the interfacial reactions between B_4C and Al, accompanied by the reaction between Mg and the oxides, occurred during hot-pressing at high temperature. The main reaction products were Al_3BC and $MgAl_2O_4$ phases. The formation of $MgAl_2O_4$, which led to severe depletion of the Mg element in the matrix, gave rise to significant degradation of the age-hardening ability of the composites.
2. The B_4C/6061Al composites with the interfacial reaction showed reduced age-hardening ability compared with 6061Al alloy, and the age-hardening ability decreased with the increase in the B_4C content, fabrication temperature and holding time. 580 °C was the optimal fabrication temperature to gain the best strength after aging treatment.
3. The age-hardening ability increased with the increase of the Mg content in the matrix. The increase rate first accelerated and then slowed down.
4. For the 20 wt%B_4C/6061Al composites hot pressed at 620 °C, the modified hot-pressing holding time and additional Mg content were 30 min and 1.5 wt%, respectively.

Acknowledgments

The authors gratefully acknowledge the support of the National Basic Research Program of China under Grant no. 2012CB619600.

References

[1] T.W. Clyne, P.J. Withers, An Introduction to Metal Matrix Composites, Cambridge University, 1993.
[2] D.J. Lloyd, Int. Mater. Rev. 39 (1994) 1–23.
[3] K.B. Lee, H.S. Sim, S.Y. Cho, H. Kwon, Mater. Sci. Eng. A 302 (2001) 227–234.
[4] J.C. Viala, J. bouix, G. Gonzalez, C. Esnouf, J. Mater. Sci. 32 (1997) 4559–4573.
[5] J. Abenojar, F. Velasco, M.A. Martínez, J. Mater. Proc. Technol. 184 (2007) 441–446.
[6] P.C. Kang, Z.W. Cao, G.H. Wu, J.H. Zhang, D.J. Wei, L.T. Lin, Int. J. Refract. Met. H 28 (2010) 297–300.
[7] D. Aidun, P. Martin, J. Sun, J. Mater. Eng. Perform. 1 (1992) 615–624.
[8] P. Jin, B.L. Xiao, Q.Z. Wang, Z.Y. Ma, Y. Liu, S. Li, Mater. Sci. Eng. A 528 (2011) 1504–1511.
[9] P. Appendino, C. Badini, F. Marino, A. Tomasi, Mater. Sci. Eng. A 135 (1991) 275–279.
[10] C. Badini, F. Marino, A. Tomasi, J. Mater. Sci. 26 (1991) 6279–6287.
[11] I. Dutta, D.L. Bourell, Mater. Sci. Eng. A 112 (1989) 67–77.
[12] M.P. Thomas, J.E. King, J. Mater. Sci. 29 (1994) 5272–5278.
[13] E.P. Hunt, P.J. Gregson, P.D. Pitcher, C.J. Peel, Scr. Metal. Mater. 25 (1991) 2769–2774.
[14] G. Gonzalez, L. Salvo, M. Suery, G. Lesperance, Scr. Metal. Mater. 33 (1995) 1969–1975.
[15] H.S. Chu, K.S. Liu, J.W. Yeh, Scr. Mater. 45 (2001) 541–546.
[16] Y.D. Huang, N. Hort, H. Dieringa, K.U. Kainer, Y.L. Liu, Acta Mater. 53 (2005) 3913–3923.
[17] H. Ribes, M. Suery, G. Lesperance, J.G. Legoux, Mater. Sci. Eng. A 21 (1990) 2489–2496.
[18] H.M. Hu, E.J. Lavernia, W.C. Harrigan, J. Kajuch, S.R. Nutt, Mater. Sci. Eng. A 297 (2001) 94–104.
[19] L. Salvo, M. Suery, Mater. Sci. Eng. A 177 (1994) 19–28.
[20] J.T. Wang, M. Furukawa, Z. Horita, M. Nemoto, Y. Ma, T.G. Langdon, Metal. Mater. Trans. A 26 (1995) 581–587.
[21] Q.C. Jiang, H.Y. Wang, B.X. Ma, Y. Wang, F. Zhao, J. Alloy Compd. 386 (2005) 177–181.
[22] Q. Zhang, B.L. Xiao, Z.Y. Liu, Z.Y. Ma, J. Mater. Sci. 46 (2011) 6783–6793.
[23] A.R. Kennedy, J. Mater. Sci. 37 (2002) 317–323.